Electronic Supplementary Material (ESI) for Dalton Transactions.

Supporting Information

Porous Organic Polymers based on Cobalt Corroles for Carbon Monoxide Binding

Stéphane Brandès,*[a] Valentin Quesneau,[a] Osian Fonquernie,[a] Nicolas Desbois,[a] Virginie Blondeau-Patissier,[b] and Claude P. Gros[a]

[a] *Université de Bourgogne Franche-Comté, ICMUB (UMR CNRS 6302), 9 Avenue Alain Savary, BP 47870, 21078 Dijon, Cedex, France. E-mail: sbrandes@u-bourgogne.fr*

[b] *Department Time-Frequency, Université de Bourgogne Franche-Comté, Institut FEMTO-ST (UMR CNRS 6174), 26 Chemin de l'épitaphe, 25030 Besançon Cedex, France*

Contents

General Considerations

Chemicals and materials: Unless otherwise noted, all chemicals and solvents were purchased from Acros® Alfa Aesar®or Sigma-Aldrich®and used without further purification excepted for DMF, which was dried over 3 Å molecular sieves. Tetrakis(4-bromophenylmethane),[1] dipyrromethane **5**,[2] corroles **1**[3] and metallocorroles **3** and **4**[4] were prepared according to previously published procedures. Column chromatography purification was carried out on silica gel (Silica 60, 40-63 µm or 63-200, Aldrich®). Analytical thin-layer chromatography (TLC) was carried out using Merck silica gel 60 F-254 plates (precoated sheets, 0.2 mm thick, with fluorescence indicator F254).

Instrumentations: All the spectrometers and diffractometers were available at the "Pôle Chimie Moléculaire", the technological platform for chemical analysis and molecular synthesis (http://www.wpcm.fr) which relies on the Institute of the Molecular Chemistry of University of Burgundy and Welience™, a Burgundy University private subsidiary.

^{1}H and ^{13}C NMR spectra were acquired on Bruker Avance III Nanobay 300 MHz and Bruker Avance III 500 MHz spectrometers. Chemical shifts (δ) of proton and carbon in ^{1}H and ^{13}C NMR spectra were expressed in ppm relative to chloroform (δ_H 7.26; δ_C 77.16), DMSO (δ_H 2.50; δ_C 39.52), C_6D_6 (δ_H 7.16; δ_C 128.06) and THF-d_8 (δ_H 1.72, 3.58; δ_C 25.31, 67.21). The unambiguous assignment of signals in ^{1}H and ^{13}C NMR spectra was performed using gradient-enhanced HSQC, HMBC and COSY correlation experiments.

Solid-state ^{13}C NMR was performed on the analytical platform of Mulhouse (IS2M, Institut de Science des Matériaux de Mulhouse) on a 400 MHz Bruker Avance II spectrometer operating at magnetic field strengths of 9.4 T, corresponding to Larmor frequencies at 100.6 MHz for ^{13}C. A Bruker 4 mm double resonance HX MAS probe was used. Tetramethylsilane was used as a secondary external reference standard. ^{13}C NMR were recorded with 90° pulse length of 5.1 µs, a recycle delay of 60 or 5 s and contact time of 1 ms. The data were acquired with spinning speed of 12 kHz. Samples were prepared by crushing products to obtain a fine powder. This powder was put in a ZrO sample holder capped with Kel-F® stopper.

FTIR analyses were recorded on a BRUKER Vertex 70v. Sample consisted on pellets (3 mg of product dispersed in 200 mg of KBr and pressed at 10 tons) which were set up on a P/N 19900 sample holder purchased from Greasby Specac. FTIR spectra recorded under CO atmosphere were run on 1% dispersion of compound in KBr pellets using a Selector™ environmental chamber accessory equipped with ZnSe windows. Baseline were recorded on a pellet of pure KBr (200 mg). Spectra were collected in the range of 400−4000 cm^{-1} at a resolution of 4 cm^{-1}.

Mass determination was run on a BRUKER Ultraflex II spectrometer in the MALDI/TOF reflectron mode using dithranol as matrix. High-resolution mass spectra (HRMS) were recorded LTQ Orbitrap XL (Thermo) instrument in the ESI mode and low-resolution mass spectra (LRMS) were run on a BRUKER Amazon SL equipped with an ionic trap and an electrospray ionization (ESI) source.

UV-visible spectra in solution were recorded on a Cary 50 spectrophotometer. All solvent used were of analytic grade. Quartz cells with optical path from 1 mm to 10 mm were used. Standard linear method using at least four different concentrations was used to determine molar extinction coefficients of corrole compounds.

UV-visible spectra in the solid-state were carried out in a diffuse reflectance mode on a Cary 5000 spectrophotometer equipped with a DRA2500 LABSPHERE integration sphere. Sample were prepared using barium sulfate as a dispersion matrix.

The CHN elemental analyses were performed on a FTA/Thermofinnigan Flash 1112 analyzer. Metal ions analyses were also achieved on a ICP-AES iCAP 7400 of the digested materials in concentrated HNO_3.

Thermogravimetric (TGA) analyses were recorded using a Netzsch STA 409 PC thermal analyzer. The samples were heated from 298 to 1273 K with a heating rate of of 5 K min^{-1} in the 298-873 K range and 10 K min^{-1} in the 873-1273 K range under a flow of nitrogen (30 mL min^{-1}) and oxygen (10 mL min^{-1}).

Nitrogen adsorption/desorption isotherms were measured at 77 K on a Micromeritics ASAP 2020 instrument. The residual solvent molecules trapped inside the pores of the solids was then removed by degassing the samples (60 – 80 mg), transferred in a pre-weighed glass, in a dynamic vacuum ($< 5 \times 10^{-3}$ Torr) at 298 K for at least 3 h before measurements. The specific surface area was determined using the Langmuir and the Brunauer−Emmett−Teller (BET) calculations, and the pore volume were obtained directly from the N_2 adsorption/desorption isotherms at $P/P_0 = 0.99$. To avoid large discrepancies between the two values of the surface area due to the invalid BET assumption for microporous solids over the usual range $0.05 < P/P_0 < 0.25$, a suitable pressure range was being applied using a range that gives increasing values of $V_{N2}(P_0–P)$ with P/P_0 as required by the groups of Snurr[5] and Rouquerol.[6] Based on the consistency of this criteria, the pressure range used for the BET surface area calculations was then $8\ 10^{-3} < P/P_0 < 0.1$. The pore size distribution of the materials was determined from the nitrogen adsorption isotherms using non-local density functional theory (NLDFT).

Low-pressure gas adsorption measurements for CO_2, N_2, and CO at 298 K were run on the same apparatus. The sample temperature was maintained using a Lauda cooler circulator and a double circulating jacket connected to a thermostatic bath in which the sample tube was dipped.

Scanning Electron Microscopy (SEM) pictures and EDS analyses were measured on a JEOL JSM 7600F microscope. Transmission Electron Microscopy (TEM) measurements were performed using a JEOL JEM 2100F microscope operating at 200 kV (point to point resolution of 0.19 nm). The samples were dispersed in ethanol and one drop of this suspension was casted on a carbon-coated copper grid. Several tens particles were counted in order to calculate nanotubes average dimensions. These microscopes are available at the ARCEN platform belonging to the “Laboratoire Interdisciplinaire Carnot de Bourgogne” (ICB).

Synthesis of starting compounds

Synthesis of Tetrakis(4-ethynylphenyl)methane 2

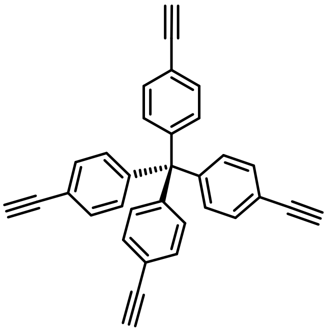

Chemical Formula: $C_{33}H_{20}$

Exact Mass: 416.1565

Molecular Weight: 416.5230

The compound was synthesized following a slightly modified procedure described in the literature.[1]

In a two neck round bottomed flask were added tetrakis(4-bromophenyl)methane[1] (5.09 g, 8.0 mmol), bis(triphenylphosphine)palladium(II) dichloride (771 mg, 1.1 mmol), copper iodide (76.0 mg, 0.4 mmol) and triphenylphosphine (1.26 g, 4.8 mmol). Solids were degassed and argon-saturated triethylamine (18 mL) and toluene (35 mL) were added under argon atmosphere. Trimethylsilylacetylene (11.3 mL, 81 mmol) was added and the reaction stirred at 80°C overnight. The solution was then cooled at room temperature, washed two times with a 1 M HCl aqueous solution and the organic phase was dried over $MgSO_4$ and evaporated under vacuum. The crude mixture was then dissolved in DCM (100 mL), poured in a round bottomed flask and a solution of sodium hydroxide (3.2 g, 81 mmol) in methanol (50 mL) was added. The reaction mixture was stirred at room temperature during 3 h, washed three times with water and the organic phase was dried over $MgSO_4$. The crude product was chromatographed on a silica gel column (DCM:heptane 1:4). Fractions containing the product were evaporated and redissolved in DCM. Methanol was added and DCM was removed slowly in vacuum to afford a crystalline white powder.

Yield: 31% (1.02 g).

^{1}H NMR (500 MHz, $CDCl_3$) δ(ppm) 7.29 (d, $^{3}J_{H-H} = 8.5$ Hz, 8H), 7.02 (d, $^{3}J_{H-H} = 8.5$ Hz, 8H), 2.96 (s, 4H).

^{13}C NMR (126 MHz, $CDCl_3$) δ(ppm) 146.20 (C_{Ar}), 131.66 (CH_{Ar}), 130.75 (CH_{Ar}), 120.29 (C_{Ar}), 83.17 (Ar-C≡C-H), 77.63 (Ar-C≡C-H), 64.80 (C-Ar).

Elementary analysis (%) calculated for $C_{33}H_{20}$ •1.1 H_2O: C 90.84, H 5.13; found: C 90.59, H 4.58.

FTIR: 3283 cm^{-1} (ν(CC—H)), 2108 cm^{-1} (ν_s(C≡CH)).

Synthesis of 5-(4-iodophenyl)dipyrromethane 5

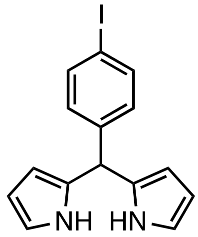

Chemical Formula: $C_{15}H_{13}IN_2$

Exact Mass: 348.0123

Molecular Weight: 348.1875

In an erlenmeyer were added 4-iodobenzaldehyde (20.0 mmol) and pyrrole (139 mL, 2.00 mol) and the mixture was degassed by a stream of nitrogen for 10 min. $MgBr_2$ (1.84 g, 10.0 mmol) was added, and the mixture was stirred for 1.5 h at room temperature. The brown mixture was treated with NaOH powder (4.0 g, 100 mmol), stirred for 1 h and then filtered on Celite®. The filtrate was concentrated, and the pyrrole was recovered. Traces of pyrrole were removed by dissolving the oil in a mixture of ethyl acetate and heptane (400 mL, 1:1) and the volatiles were removed. The solid was recrystallized in a DCM:heptane mixture affording a yellow powder.

Yield: 92% (6.42 g)

^1H NMR (500 MHz, DMSO-d_6) δ(ppm) 10.55 (s, 2H), 7.71-7.57 (m, 2H), 7.06-6.92 (m, 2H), 6.62 (m, 2H), 5.91 (m, 2H), 5.66 (m, 2H), 5.33 (s, 1H).

^{13}C NMR (126 MHz, $CDCl_3$) δ(ppm) 142.0 (Cq), 137.8 (CH), 131.9 (Cq), 130.5 (CH), 117.6 (CH), 108.7 (CH), 107.6 (CH), 92.5 (CI), 43.7 (CH-*meso*).

MS (ESI): m/z 346.7 $[M-H]^-$, 347.0 calcd for $C_{15}H_{12}IN_2$.

Elementary analysis (%) calculated for $C_{15}H_{13}IN_2$: C 51.89, H 3.74, N 8.07; found: C 51.89, H 3.96, N 8.24.

Synthesis of free base corrole and complexes

Synthesis of 10-Phenyl-5,15-(4-iodophenyl)corrole 1

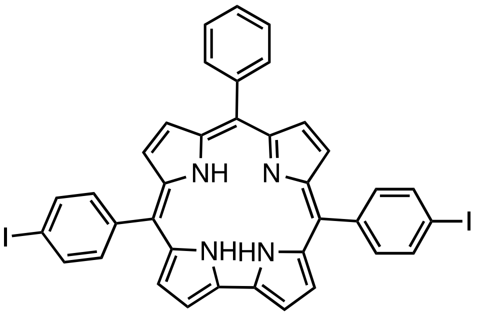

Chemical Formula: $C_{37}H_{24}I_2N_4$

Exact Mass: 778.0090

Molecular Weight: 778.4359

5-(4-iodophenyl)dipyrromethane **5** (8.0 mmol) and benzaldehyde (4.0 mmol, 0.5 eq) were dissolved in 800 mL of methanol. Then, a solution of HCl (36%, 20 mL) in H_2O (400 mL) was added, and the reaction mixture was stirred at room temperature for 1 hour. The mixture was extracted with chloroform and the organic phase was washed three times with water, dried and completed to 2 L *p*-chloranil (1 eq) was added and the reaction mixture was stirred overnight at room temperature protected from the light and the solution was evaporated. Hydrazine monohydrate (10 mL) was added to the solution and stirred during 30 minutes before evaporation of the mixture to reduce corrole radical formed during the oxidation step. The solution was filtered on Celite® and the filtrate was evaporated. The crude mixture was chromatographed on a silica gel plug (DCM:heptane 4:1) and fractions containing corrole were collected and evaporated. The residue was dissolved in DCM, ethanol was then added and DCM was removed in vacuum, affording the crystallization of the product.

Yield: 26% (802 mg).

^1H NMR (500 MHz, DMSO-d_6 + 5% $NH_2NH_2 \bullet H_2O$) δ(ppm) 8.94 (d, $^3J_{H-H}$ = 3.9 Hz, 2H), 8.63 (d, $^3J_{H-H}$ = 4.5 Hz, 2H), 8.51 (d, $^3J_{H-H}$ = 3.9 Hz, 2H), 8.30 (d, $^3J_{H-H}$ = 4.5 Hz, 2H), 8.15 (d, $^3J_{H-H}$ = 8.2 Hz, 4H), 8.10 (d, $^3J_{H-H}$ = 6.6 Hz, 2H), 8.06 (d, $^3J_{H-H}$ = 8.2 Hz, 4H), 7.74-7.64 (m, 3H).

^{13}C NMR (126 MHz, THF-d_8 + 5% $NH_2NH_2 \bullet H_2O$) δ(ppm) 141.6, 139.4, 138.8, 137.7, 135.6, 135.0, 134.9, 134.7, 134.7, 134.4, 134.0, 132.7, 130.8, 126.8, 126.1, 124.9, 124.8, 123.6, 123.3, 123.2, 122.9, 119.7, 113.5, 113.4, 111.6, 107.4, 91.1.

MS (MALDI-TOF): m/z 777.8 $[M]^{+\bullet}$, 778.0 calcd for $C_{37}H_{24}I_2N_4$.

HR-MS (MALDI-TOF): m/z 779.0153 $[M+H]^+$, 779.0163 calcd for $C_{37}H_{24}I_2N_4$.

UV-Vis (toluene): λ_{max} (nm) (ε x 10^{-3} L mol^{-1} cm^{-1}) 428 (129.8), 568 (18.7), 622 (14.7), 653 (15.0).

FTIR (KBr): 3371 cm^{-1} (ν(N–H)).

Elementary analysis (%) calculated for $C_{37}H_{24}I_2N_4 \bullet 4.3\ H_2O$: C 51.90, H 3.84, N 6.54; found: C 51.76, H 3.39, N 7.13.

Synthesis of O-sulfinylbis(methane)[10-Phenyl-5,15-(4-iodophenyl)corrolato]cobalt 4

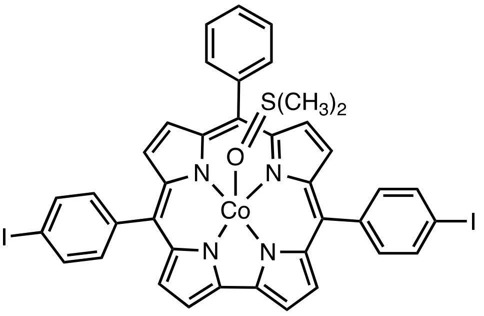

Chemical Formula: $C_{39}H_{27}CoI_2N_4OS$

Exact Mass: 911.9327

Molecular Weight: 912.4741

In a round bottom flask, a solution of free-base corrole **1** (210 mg, 0.27 mmol, 1 eq) and $Co(OAc)_2•4H_2O$ (80.7 mg, 0.32 mmol, 1.2 eq) in DMSO (80 mL) was heated to 80 °C under stirring for 40 min and then cooled at room temperature. The crude mixture was then poured into cold NaCl aqueous solution (0.8 M) and the resulting suspension was filtered. The solid was washed five times with water and dried under vacuum.

Yield: 86% (213 mg).

^{1}H NMR (500 MHz, $CDCl_3$+ 5% $NH_3•H_2O$ (25% w/w in H_2O)) δ(ppm) 9.25 (d, $^3J_{H\text{-}H}$ = 4.3 Hz, 2H), 9.03 (d, $^3J_{H\text{-}H}$ = 4.6 Hz, 2H), 8.90-8.80 (m, 4H), 8.24 (d, $^3J_{H\text{-}H}$ = 7.2 Hz, 2H), 8.13 (d, $^3J_{H\text{-}H}$ = 8.0 Hz, 4H), 8.08 (d, $^3J_{H\text{-}H}$ = 8.0 Hz, 4H), 7.75 (m, 3H), 2.63 (s, 6H), -6.79 (s, 6H).

MS (MALDI-TOF): m/z 833.7 $[M–DMSO]^{+•}$, 833.9 calcd for $C_{37}H_{21}CoI_2N_4$.

HR-MS (ESI): m/z 833.9187 $[M–DMSO]^{+•}$, 833.9182 calcd for $C_{37}H_{21}CoI_2N_4$.

UV-Vis (toluene + 1% DMSO): λ_{max} (nm) (ε x 10^{-3} L mol$^{–1}$ cm$^{–1}$) 394 (87.1), 567 (18.3).

FTIR (KBr): 987 cm$^{–1}$ (ν(S=O), bound sulfoxide).

Elementary analysis (%) calculated for $C_{39}H_{27}CoI_2N_4OS•2H_2O$: C 49.39, H 3.29, N 5.91 S 3.38; found: C 49.19, H 2.49, N 5.46, S 4.57.

Synthesis of bisammine[10-phenyl-5,15-(4-iodophenyl)corrolato]cobalt 3

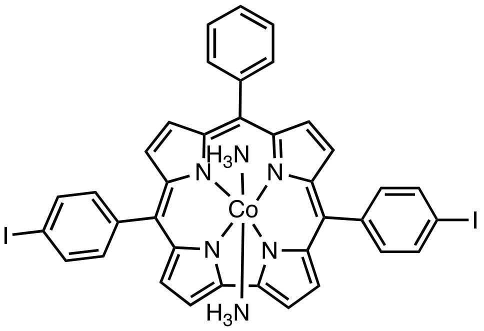

Chemical Formula: $C_{37}H_{27}CoI_2N_6$

Exact Mass: 867.9719

Molecular Weight: 868.4071

In a round bottom flask, a solution of free-base corrole **1** (389 mg, 0.50 mmol, 1 eq) and $Co(OAc)_2•4H_2O$ (137 mg, 0.55 mmol, 1.1 eq) in DMSO (150 mL) was heated to 80 °C under stirring for 40 min and then cooled at room temperature. Dichloromethane (150 mL) was then added to the solution and the organic phase was washed four times (4 x 100 mL) with an aqueous 0.4 M ammonia solution. Five drops of a 25% aqueous ammonia solution and methanol (50 mL) was added to the organic phase and dichloromethane was removed under vacuum, affording the crystallization of the desired product. The solid was then filtered, washed with methanol and dried overnight under vacuum at room temperature.

Yield: 403 mg (93%).

^{1}H NMR (500 MHz, $CDCl_3$ + 2% $NH_2NH_2 \cdot H_2O$) δ(ppm) 9.14 (d, $^3J_{H\text{-}H}$ = 4.1 Hz, 2H), 8.96 (d, $^3J_{H\text{-}H}$ = 4.7 Hz, 2H), 8.80 (d, $^3J_{H\text{-}H}$ = 4.7 Hz, 2H), 8.75 (d, $^3J_{H\text{-}H}$ = 4.1 Hz, 2H), 8.15 (d, $^3J_{H\text{-}H}$ = 6.6 Hz, 2H), 8.10 (d, $^3J_{H\text{-}H}$ = 8.2 Hz, 4H), 7.97 (d, $^3J_{H\text{-}H}$ = 8.2 Hz, 4H), 7.72 (m, 3H), –4.16 (s, 4H).

MS (MALDI-TOF): m/z 833.9 $[M–2NH_3]^{+\bullet}$, 833.9 calcd for $C_{37}H_{21}CoI_2N_4$.

HR-MS (ESI): m/z 833.9189 $[M–2NH_3]^{+\bullet}$, 833.9182 calcd for $C_{37}H_{21}CoI_2N_4$.

UV-Vis (toluene with 1% $NH_3 \cdot H_2O$ (25% w/w in H_2O): λ_{max} (nm) (ε x 10^{-3} L mol^{-1} cm^{-1}) 313 (24.5), 438 (91.3), 455 (70.7), 586 (11.9), 632 (40.2).

FTIR (KBr): 3344 cm^{-1} ($\nu_a(NH_3)$), 3254 cm^{-1}($\nu_s(NH_3)$).

Elementary analysis (%) calculated for $C_{37}H_{27}CoI_2N_6$: C 51.18, H 3.13, N 9.68; found : C 51.76, H 3.39, N 8.95.

NMR characterization of tetrahedral building block and corroles

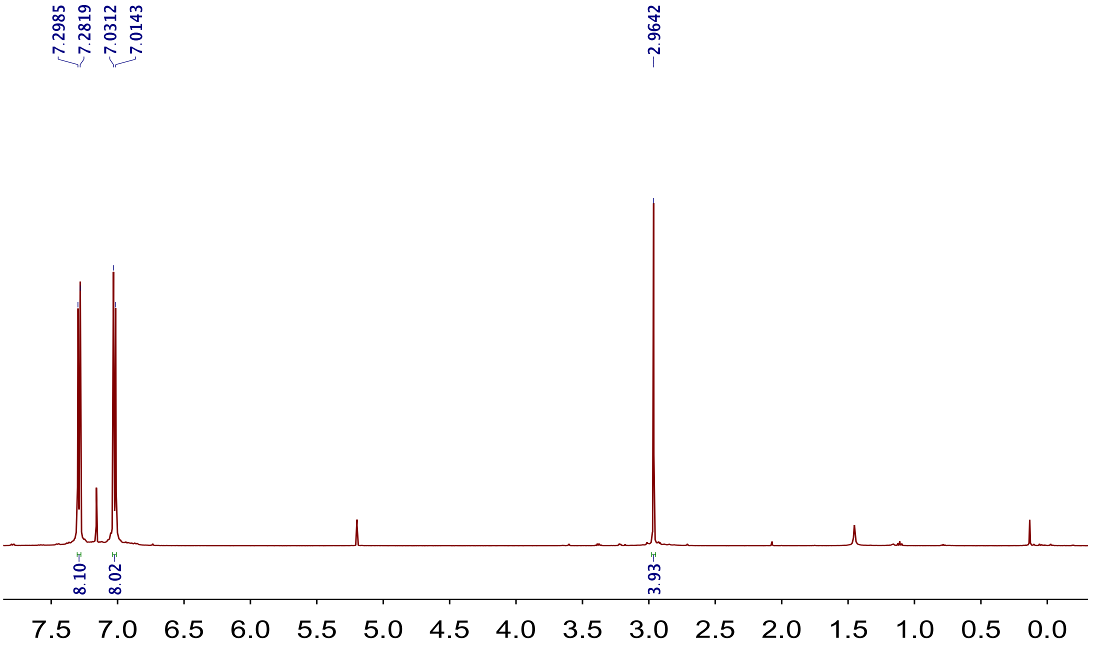

Fig. S1 ^{1}H NMR spectrum of **2** recorded in $CDCl_3$ at 298 K.

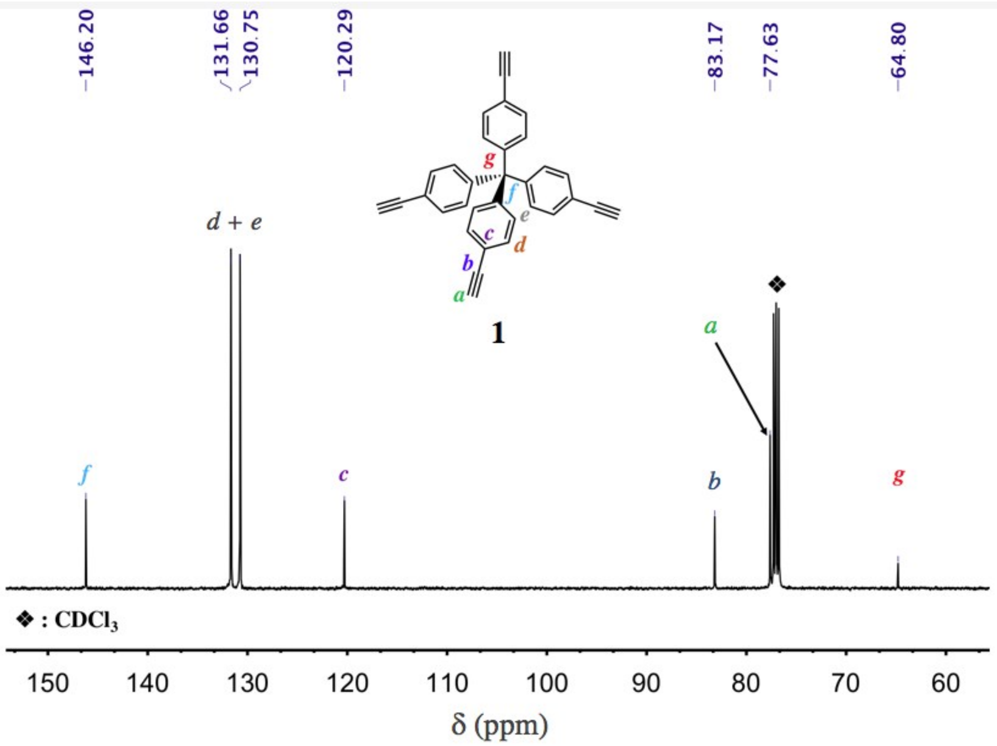

Fig. S2 $^{13}C\{^{1}H\}$ NMR spectrum of **2** recorded in $CDCl_3$ at 298 K.

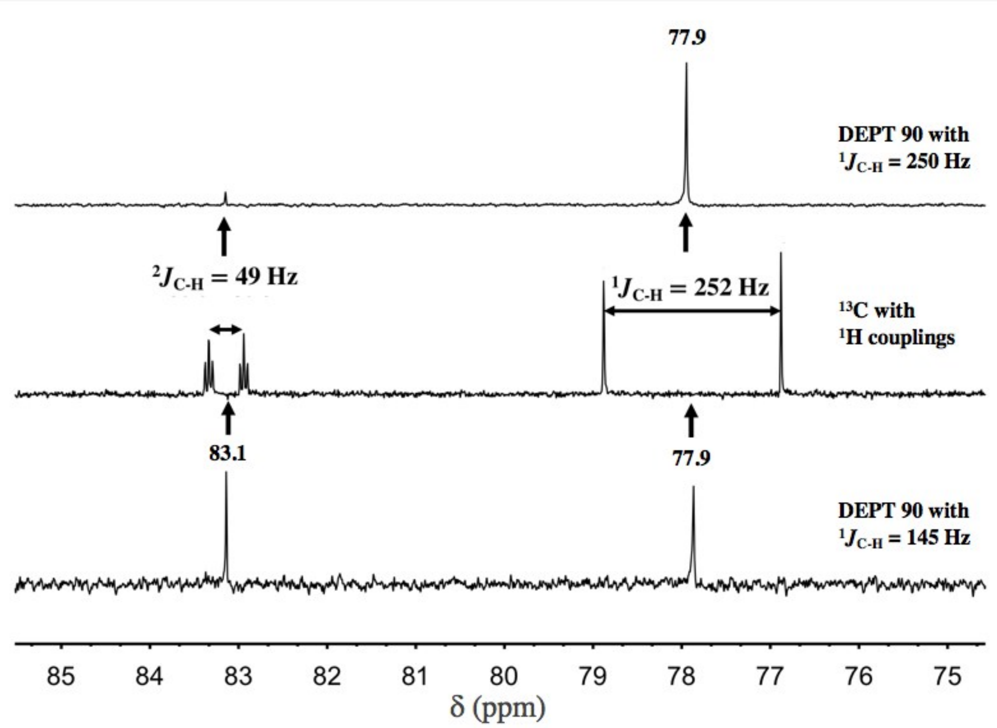

Fig. S3 Proton-coupled ^{13}C and DEPT-90 NMR spectra of **2** using decoupling constant equal to 145 and 250 Hz, shown in the alkyne region. Spectra were recorded in $CDCl_3$ at 298 K.

The $^{13}\mathrm{C}\{^{1}\mathrm{H}\}$ NMR spectrum of the tetrahedral precursor **2** in solution in $CDCl_3$ shows 7 peaks (Fig. S2). The resonance signal at 64.8 ppm is characteristic of the quaternary methine carbon atom. The two signals at 77.9 and 83.1 ppm correspond to the carbon atoms of the alkyne function. In order to discriminate the two alkyne carbon atoms, a DEPT-90 experiment was performed in order to reveal only the carbon atoms with sp hybridization. On the spectrum, two signals of the same phase are observed at 77.9 and 83.1 ppm (Fig. S3). This result is unexpected because the quaternary carbon atoms of the alkyne function should not give any signal in DEPT 90 experiments. This result can be explained by the value of the discrepancy between the predefined $^{1}J_{\text{C-H}}$ coupling for the DEPT experiment (default value: 145 Hz) and the real $^{1}J_{\text{C-H}}$ coupling for terminal alkyne, which is about 250 Hz.[7-9]

The simplest NMR experiment that can be used to discriminate between the two carbon atoms of the alkyne is a proton-coupled ^{13}C NMR experiment (Fig. S3). A doublet centered at 77.9 ppm and a triplet-doublet at 83.1 ppm are clearly observed with coupling constants of 252, 49 and 5.3 Hz, respectively. The first value value is characteristic of $^{1}J_{\text{C-H}}$ coupling for a terminal alkyne, although 49 Hz value is in perfect agreement with $^{2}J_{\text{C-H}}$ coupling constant between the terminal alkyne proton and the quaternary carbone atom (C_b-H_a coupling). The observed triplet corresponds to $^{3}J_{\text{C-H}}$ coupling with aryl protons (*d*).

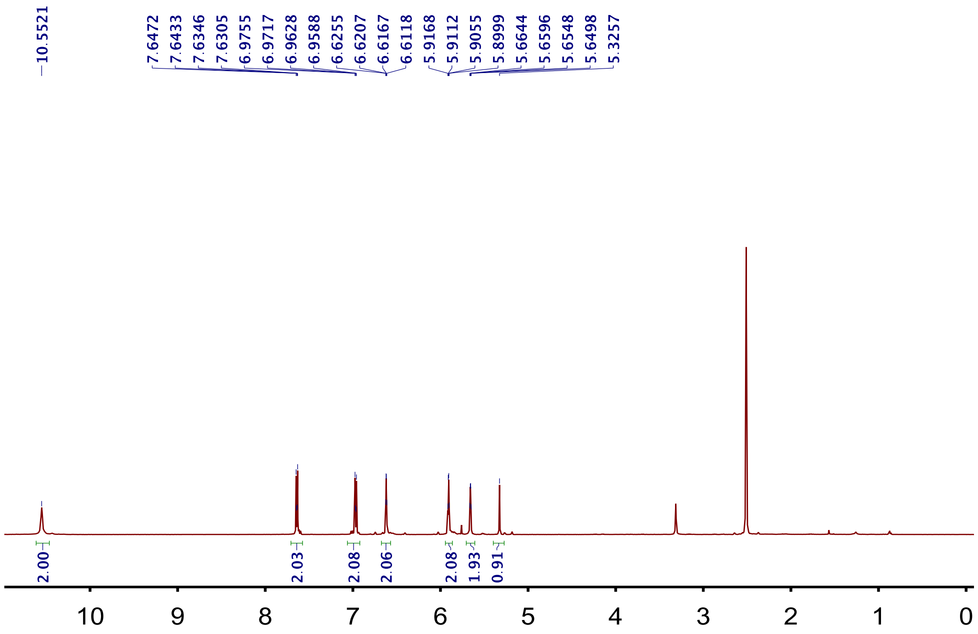

Fig. S4 ^{1}H NMR spectrum of dipyrromethane **5** recorded in DMSO-d_6 at 298 K.

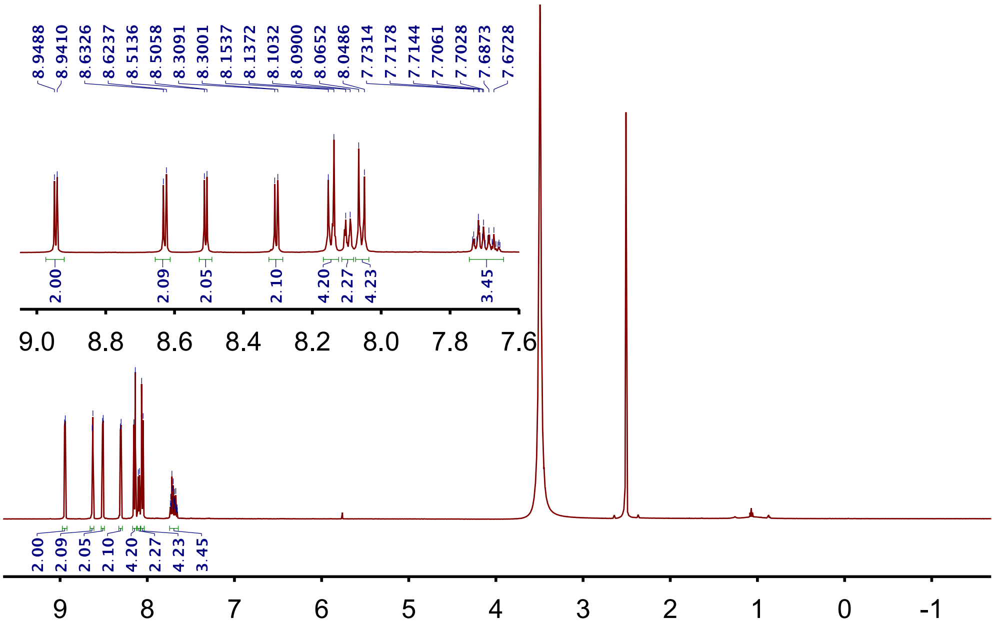

Fig. S5 ^{1}H NMR spectrum of free base corrole **1** recorded in DMSO-d_6 at 298 K.

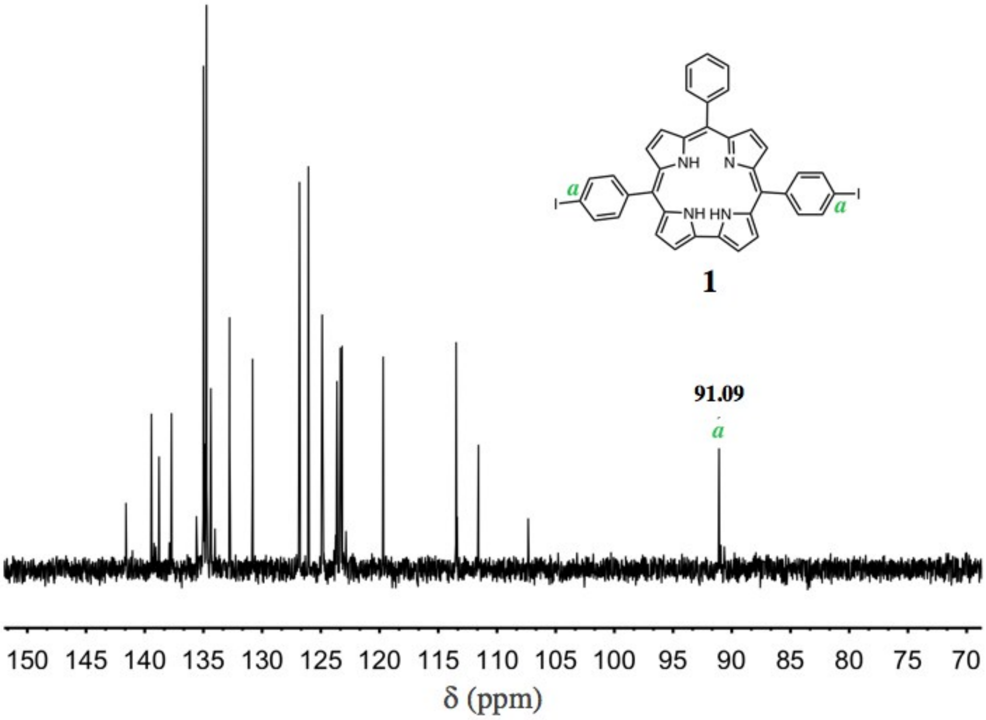

Fig. S6 $^{13}C\{^{1}H\}$ NMR spectrum of **1** recorded in THF-d_8 at 298 K.

The $^{13}C\{^{1}H\}$ NMR spectrum of corrole **1** dissolved in deuterated toluene shows numerous peaks between 110 and 140 ppm corresponding to the aromatic carbon atoms (Fig. S6). The signal at 91.09 ppm corresponds to carbon atoms bound to the iodine atoms is clearly observed. This signal is shielded from other aromatic carbon atoms because of the heavy atom effect of iodine.[10,11] The presence or absence of this signal can be further exploited to highlight the polymerization level of the materials.

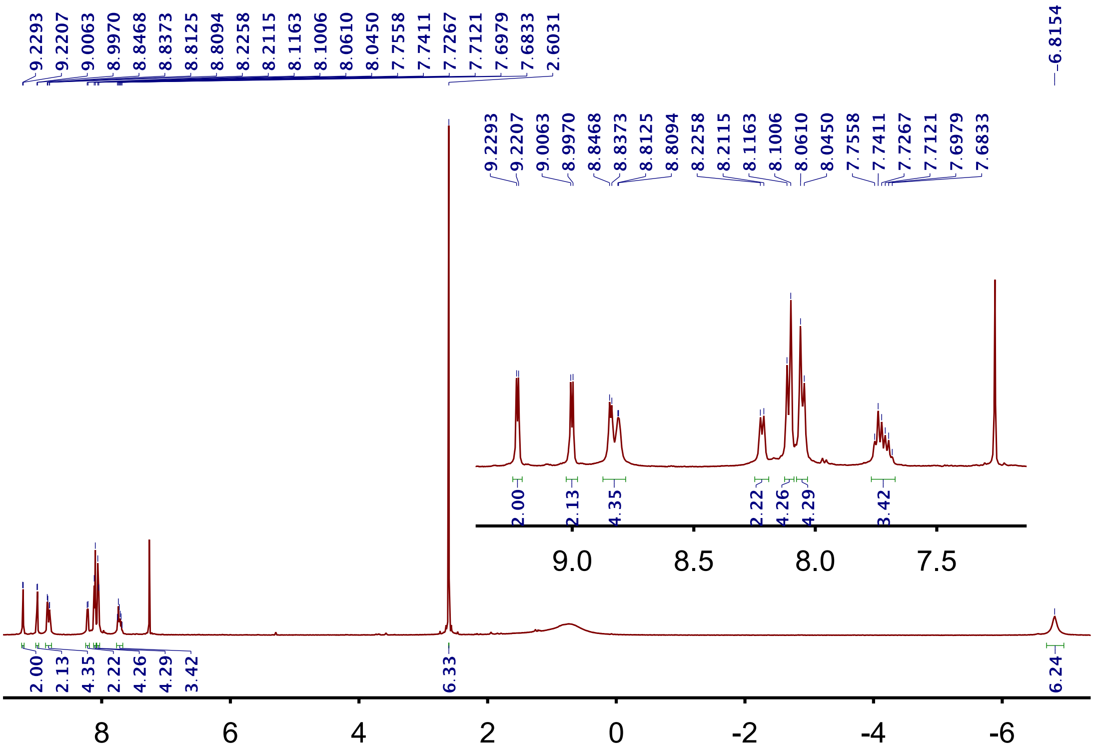

Fig. S7 ^{1}H NMR spectrum of **4** recorded at 298 K in $CDCl_3$ + 5% $NH_3 \cdot H_2O$.

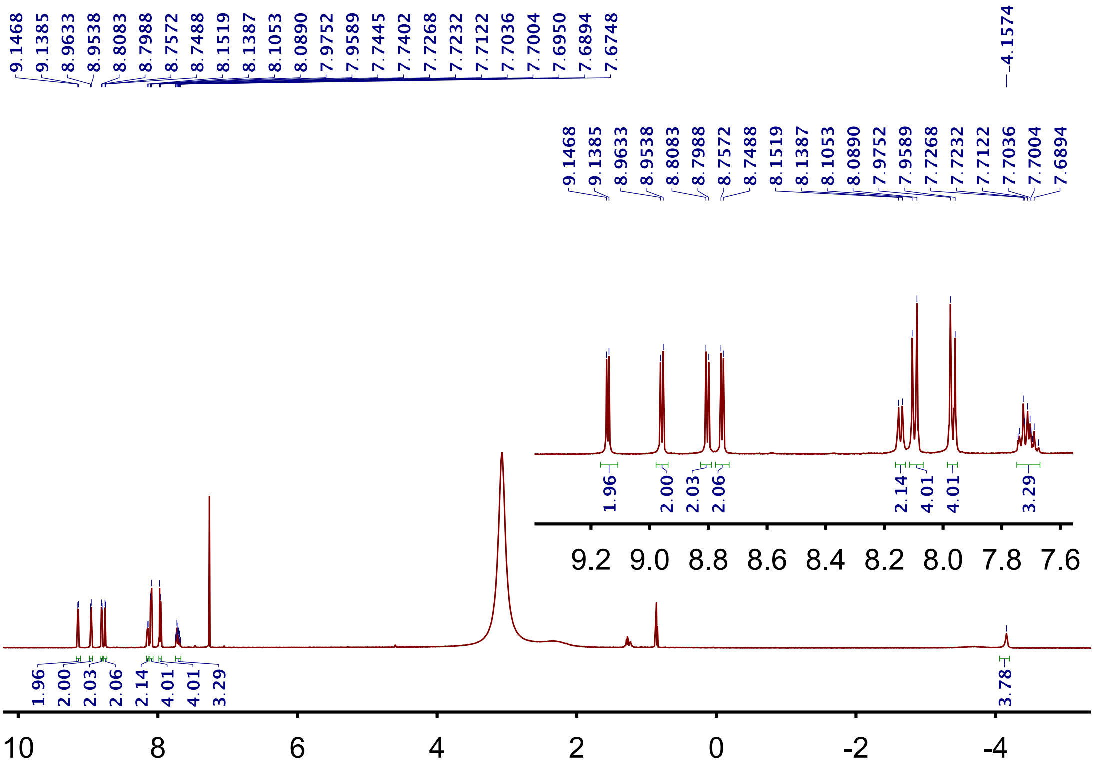

Fig. S8 ^{1}H NMR spectrum of **3** recorded at 298 K in $CDCl_3$ + 2% $NH_2NH_2 \cdot H_2O$.

Synthesis of materials

POP-Cor

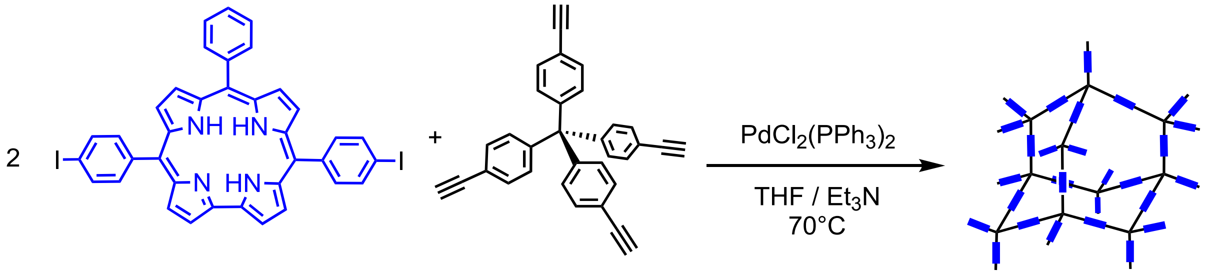

1 **2**

In a two-necked round bottom flask was added under inert atmosphere corrole **1** (100 mg, 0.128 mmol, 1 eq), dry tetrahydrofuran (40 mL), dry triethylamine (15 mL), bis(triphenylphosphine) palladium(II) dichloride (7.2 mg, 0.010 mmol, 0.04 eq per alkyne function). The mixture was then heated at 70 °C under stirring and a solution of tetra-alkyne **2** (26.7 mg, 0.064 mmol, 0.5 eq) in dry tetrahydrofuran (30 mL) was added dropwise during at least 2 h. The solution was stirred for 24 h at 70 °C. After cooling down at room temperature, the black precipitate formed was filtered, washed with tetrahydrofuran and methanol and dried under vacuum.

Yield: 78 mg (82%).

Elementary analysis (%), calculated for $C_{107}H_{63.1}N_8I_{0.9}$•6($H_2O$)•0.18(Pd): C 75.50, H 4.50, N 6.58; found: C 75.07, H 3.79, N 6.27.

FTIR (cm^{-1}): 3371 (ν(N–H)), 2204 (ν(C-C≡C-C)), 2108 (ν(C-C≡C-H)) (see Fig. S9).

ICP (%): Pd found 1.16%, corresponding to 0.18 Pd.

UV-Vis ($BaSO_4$, diffuse reflectance mode): λ_{max} (nm) 470, 603.

^{13}C NMR (CP-MAS): δ(ppm) 145 (C_{Ar}), 136 (C_{Ar}), 132 (C_{Ar}), 122 (C_{Ar}), 93 (residual C-I), 65 (C-Ar).

POP-CorCo-1

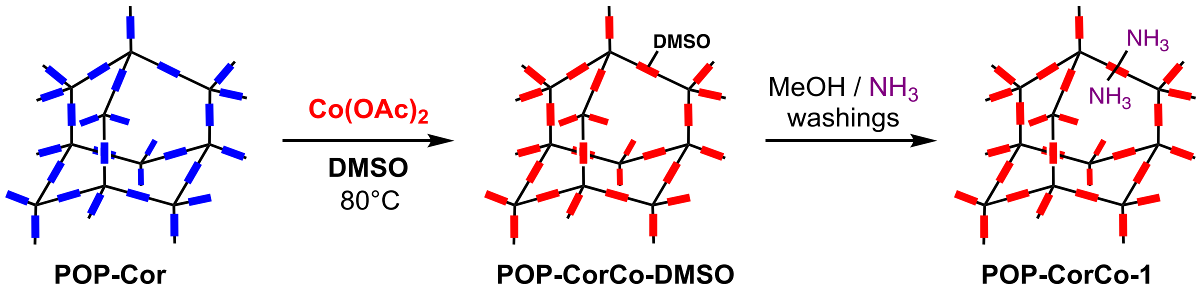

In a round bottom flask **POP-Cor** (100 mg) was degassed under vacuum for few minutes and argon-saturated DMSO (12 mL) was added under argon. A solution of cobalt acetate in DMSO (67 mg in 8 mL) was added under argon and the solution was heated under stirring during 2 h at 80 °C. After cooling down the solution, the suspension was centrifuged. The supernatant was eliminated and the solid washed with methanol to afford **POP-CorCo-DMSO**. The black powder was then washed with a solution of methanol saturated with ammonia to afford **POP-CorCo-1** coordinated by two NH_3 ligands on the cobalt center. The solid was then dried under vacuum at room temperature.

Characterization of **POP-CorCo-DMSO**:

UV-Vis ($BaSO_4$, diffuse reflectance mode): λ_{max} (nm) 467, 576.

Characterization of **POP-CorCo-1**:

Yield: 95% (104 mg).

Elementary analysis (%) calculated for $C_{107}H_{57.3}N_8Co_2I_{0.7}$•13($H_2O$)•0.17(Pd): C 67.15, H 4.42, N 5.85; found: C 67.07, H 4.02, N 5.78.

ICP calcd %Co for quantitative metalation: 6.15, found: 4.95; (% metalation = 81%); %Pd found: 0.94%, corresponding to 0.17 Pd.

FTIR (cm^{-1}): 2204 (ν(C-C≡C-C)), 2108 (ν(C-C≡C-H)) (see Fig. S9).

NH_3 content calculated by TGA: Δm (calcd. for 2 NH_3 ligand / Co) = 3.1% (2.1%), T_{onset} = 50°C, T_{end} = 166 °C.

POP-CorCo-2

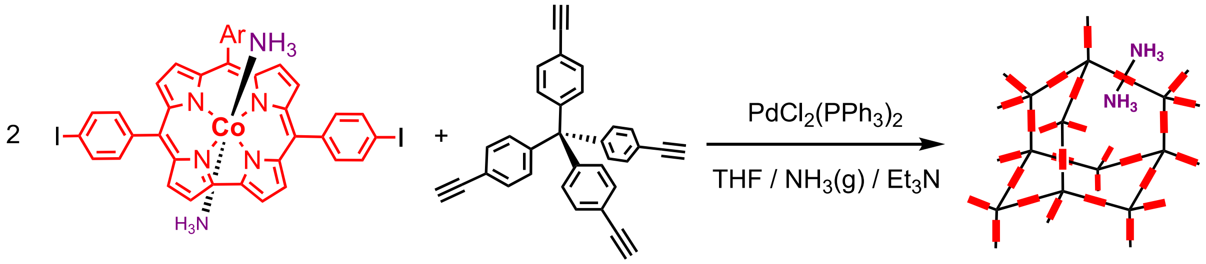

3 **2**

In a doubled-necked round bottom flask was added under inert atmosphere was dissolved cobalt corrole **3** (110 mg, 0,126 mmol, 1 eq) in tetrahydrofuran (40 mL) and gaseous ammonia was bubbling for 5 min in the solution affording a green solution. Then triethylamine (15 mL) and bis(triphenylphosphine)palladium(II) dichloride (7.1 mg, 0.010 mmol, 0.1 eq) were added. The mixture was heating under stirring at 70 °C and a solution of tetra-alkyne **2** (26.3 mg, 0.063 mmol, 0.5 eq) in tetrahydrofuran (30 mL) was added dropwise during at least 2 h. The solution was then allowed to stir for 24 h at 70 °C. After cooling down at room temperature, the black precipitate formed was filtered, washed with tetrahydrofuran followed by a saturated ammonia solution in tetrahydrofuran. The black solid was dried under vacuum.

Yield: 70% (70 mg).

Elementary analysis: Calculated for $C_{107}H_{57}N_8Co_2I \cdot 11(H_2O) \cdot 0.19(Pd)$: C 66.98, H 4.25, N 5.84; found: C 67.02, H 3.93, N 5.94.

ICP calcd %Co: 6.14, found: 5.21; %Pd found: 1.03, corresponding to 0.19 Pd.

FTIR (cm^{-1}): 2204 (ν(C-C≡C-C)), 2108 (ν(C-C≡C-H)) (see Fig. S9).

UV-Vis ($BaSO_4$): λ_{max} (nm) 467, 605, 667.

NH_3 content by TGA: Δm (calcd. for 2 NH_3 ligated) = 3.0% (2.1%), T_{onset} = 60 °C, T_{end} = 150 °C.

Characterization of materials

FTIR spectroscopy

a)

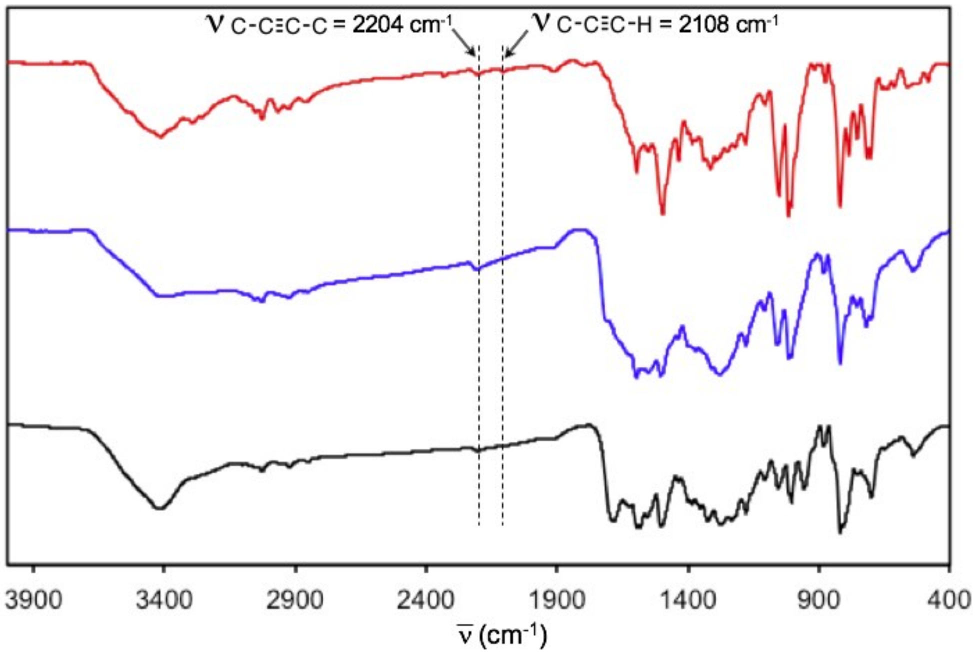

b)

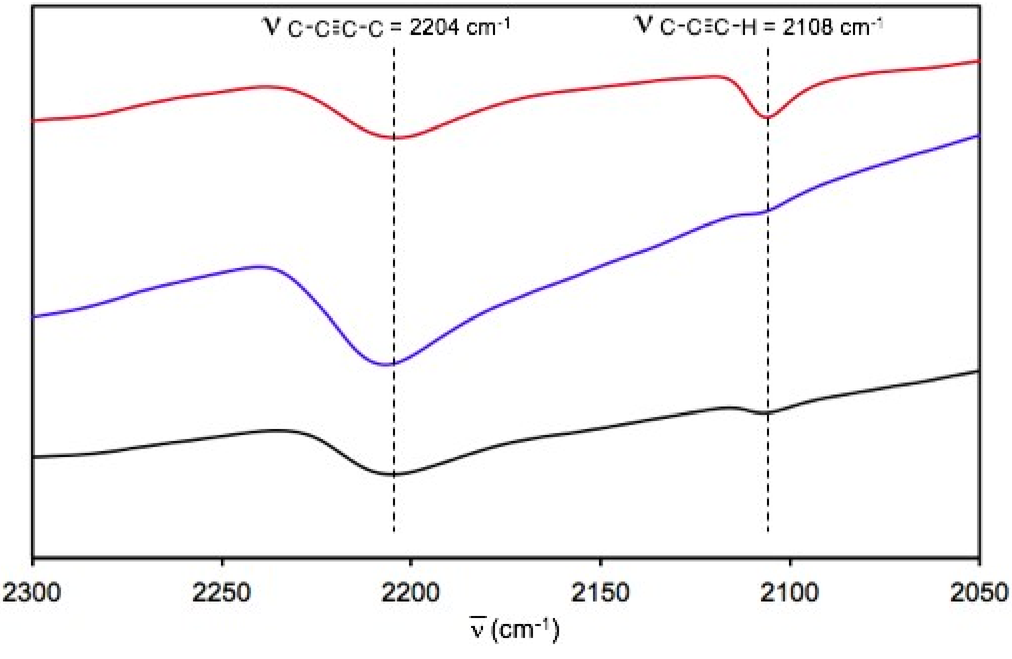

Fig. S9 (a) FTIR spectra of **POP-CorCo-2** (red line), **POP-CorCo-1** (blue line) and **POP-Cor** (black line) recorded in transmission with KBr pellets; (b) Expanded part in the alkyne region.

UV-visible in diffuse reflectance mode

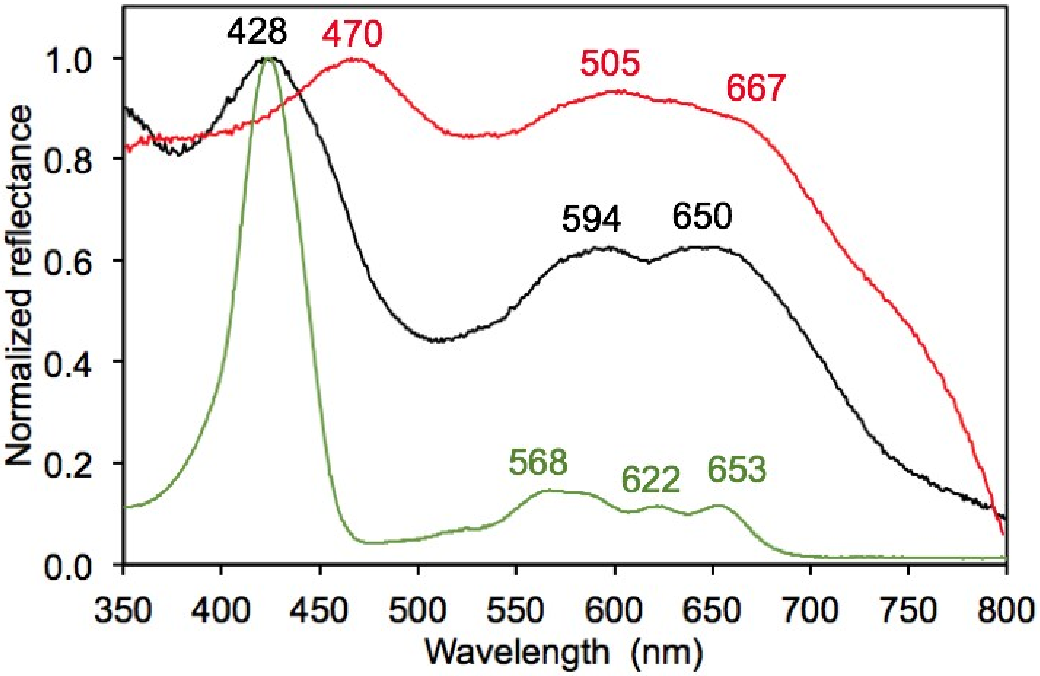

Fig. S10 UV-visible spectra for free base corrole **1** recorded in toluene solution (green line) and in solid state (black line), and for **POP-Cor** (red line).

Microscopy analyses

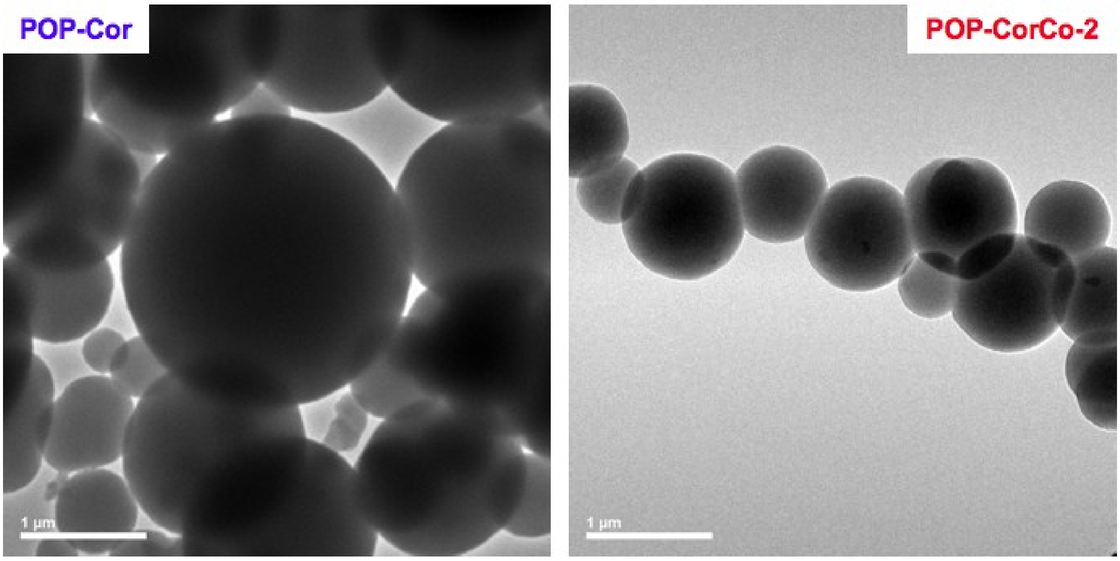

Fig. S11 TEM images of **POF-Cor** (left) **POP-CorCo-2** (right).

Chemical composition determined by EDS, ICP and elementary analyses

Table S1 Atomic ratios for different elements calcultated from the EDS analyses

Material	%N / %Co	%Co / %I	%P / %Pd
POP-Cor	nd[a]	nd[a]	2.0
POP-CorCo-1	2.53	3.00	1.0
POP-CorCo-2	2.00	1.20	2.0

[a] Non determined

Thermogravimetric analyses

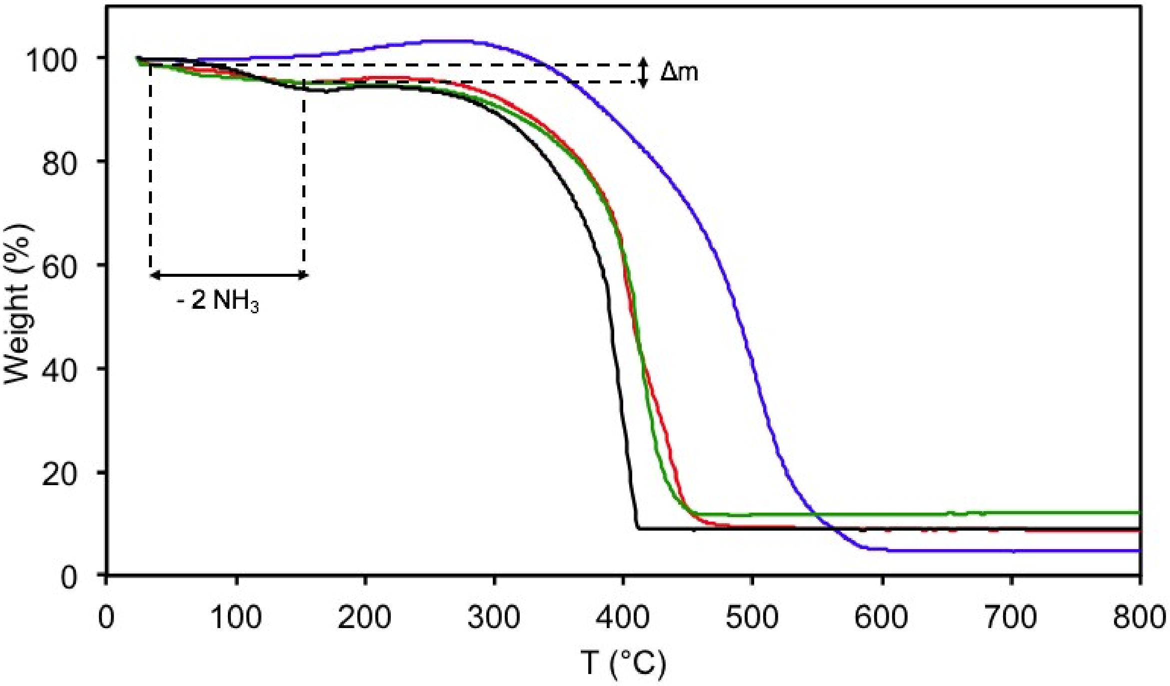

Fig. S12 Thermogravimetric analyses recorded for corrole **3** (black curve), **POP-Cor** (blue curve), **POP-CorCo-1** (green curve) and **POP-CorCo-2** (red curve) under a N_2/O_2 gas flow.

Table S2 Thermogravimetric data for the cobalt-complexed POPs.

Material	Δm (%)	Δm_{theo}[a] (%)	T_{end} (°C)	%CoO exp (calcd)[b]
POP-CorCo-1	3.1	2.1	166	12.0 (9.3)
POP-CorCo-2	3.0	2.1	150	8.3 (9.3)

[a] Considering two NH_3 per cobalt atom. [b] Based on the estimated molecular formulas.

Gas adsorption analyses

Porosity of the polymers

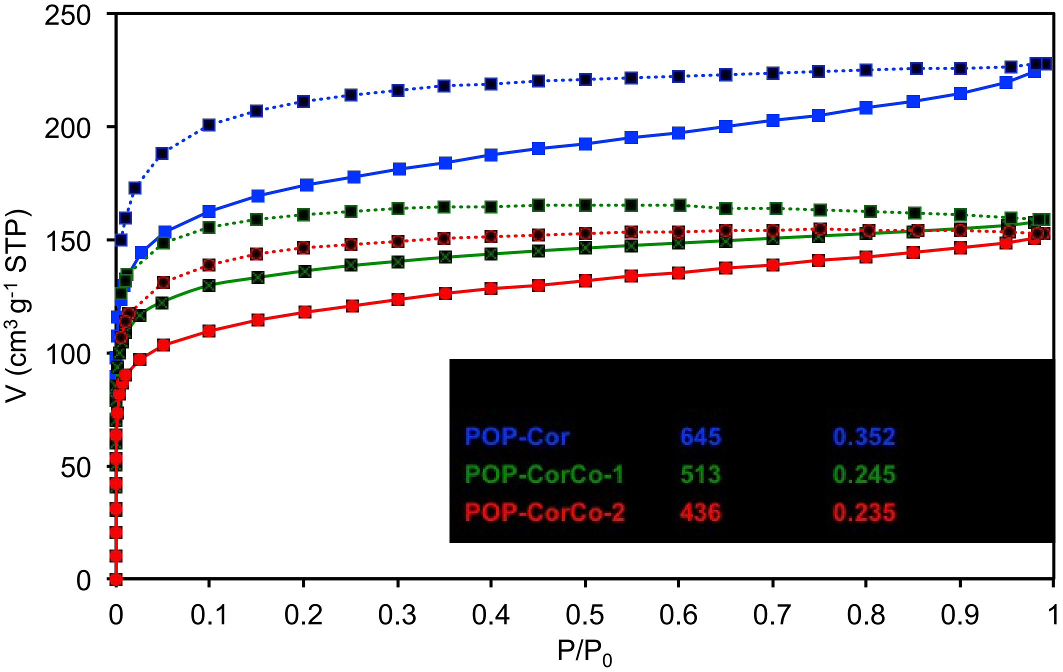

Fig. S13 N_2 adsorption (closed symbols) and desorption (open symbols) isotherms recorded at 77 K for **POP-Cor** (blue square), **POP-CorCo-1** (green square) and **POP-CorCo-2** (red circles).

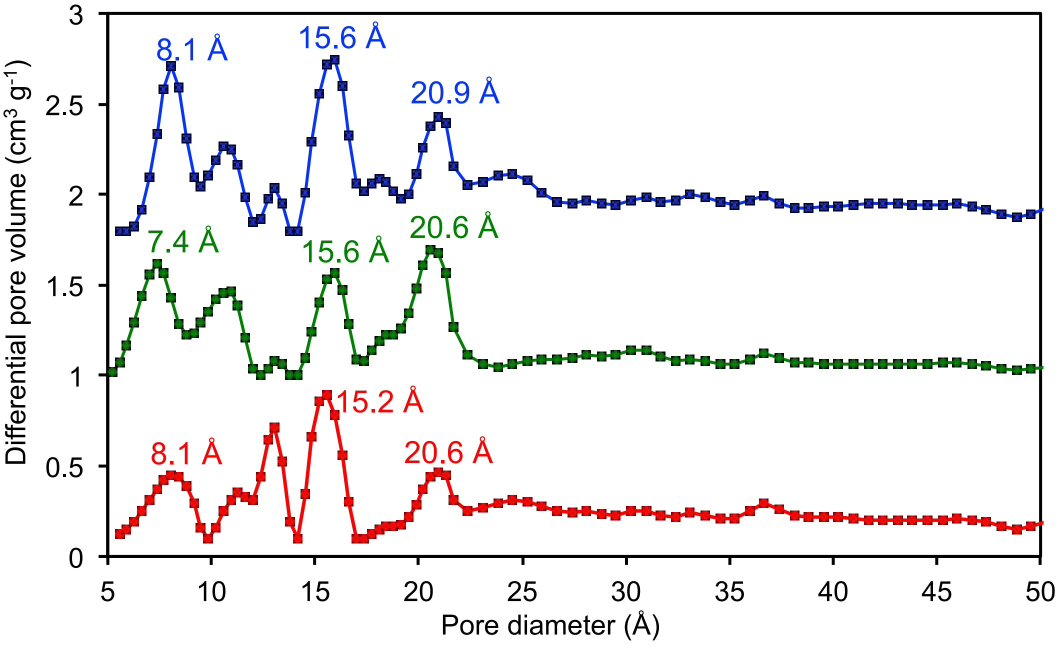

Fig. S14 Pore size distribution curves of **POP-Cor** (blue curve), **POP-CorCo-1** (green curve) and **POP-CorCo-2** (red curve) calculated from N_2 adsorption isotherms at 77 K using NLDFT method.

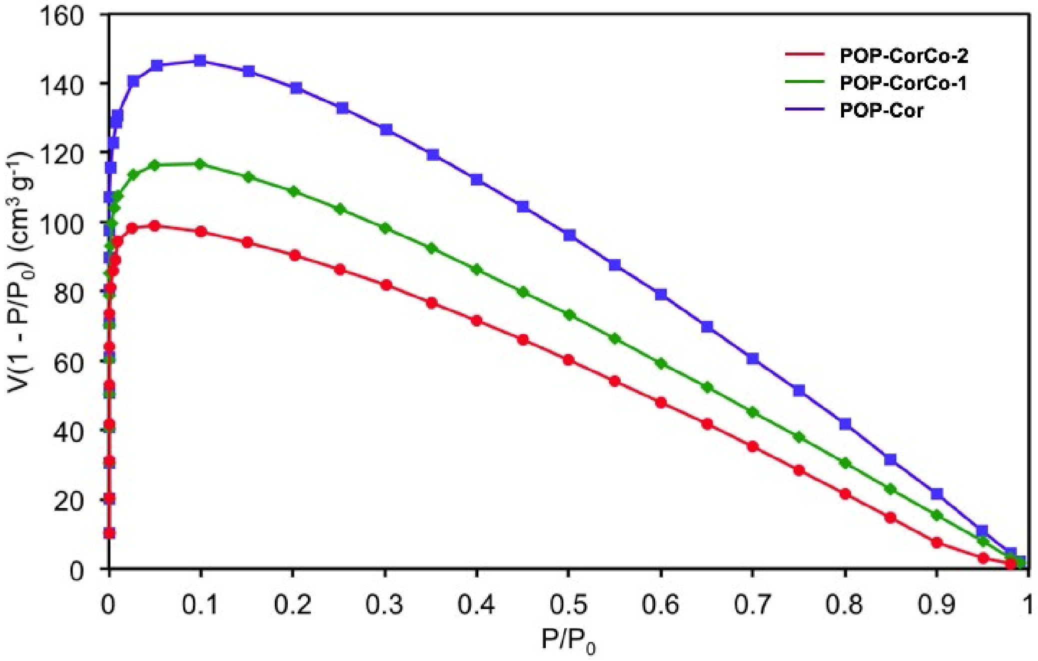

Fig. S15 Rouquerol plots[6] for materials **POP-Cor**, **POP-CorCo-1** and **POP-CorCo-2** to determine the pressure range validity of the BET equation. Plots lead to the selection of the appropriate relative pressure range of 0.006 – 0.100 for all materials.

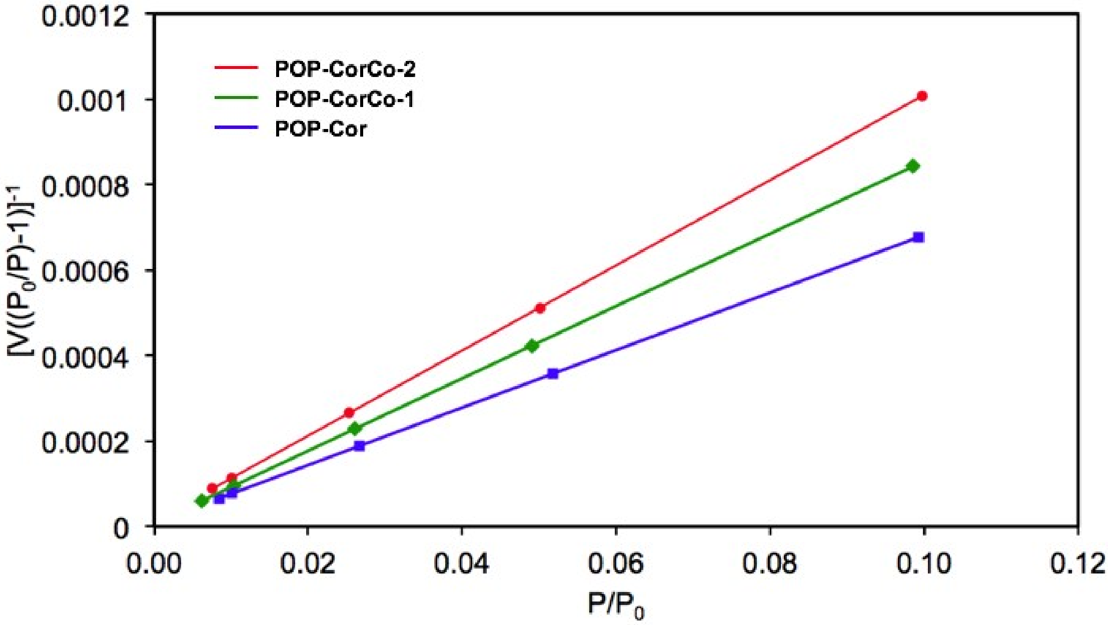

Fig. S16 BET plots for **POP-Cor**, **POP-CorCo-1** and **POP-CorCo-2** using the pressure range defined by the Rouquerol recommendations[6] on Fig. S15.

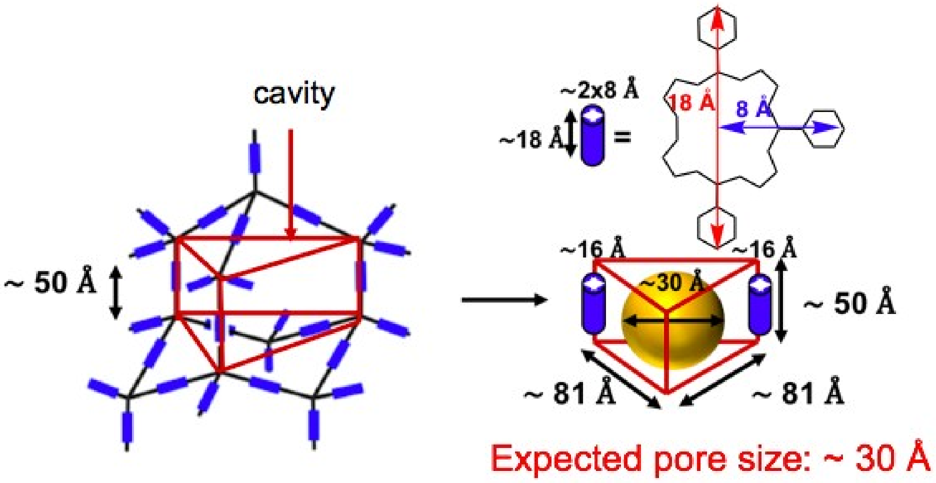

Fig. S17 Estimation of the cavity size considering a regular diamond topology of the framework.

Models for isotherm fitting

The Langmuir model is applicable only to monolayer adsorption on a homogeneous surface with a finite number of binding sites with same energy. In the case of **POP-CorCo-1 and -2**, experimental single gas adsorption isotherms for CO_2, N_2 and O_2 were fit using a single-site (1) and a triple-site (2) Langmuir equation:

Single-site Langmuir equation:
$$V_{ads}^{i} = \frac{V_1 K_1 P}{1 + K_1 P} \tag{1}$$

Triple-site Langmuir equation:
$$V_{ads}^{i} = \frac{V_1 K_1 P}{1 + K_1 P} + \frac{V_2 K_2 P}{1 + K_2 P} + \frac{V_3 K_3 P}{1 + K_3 P} \tag{2}$$

where V_{ads} is the total amount adsorbed in $cm^3\ g^{-1}$, P is the applied pressure in atm, V_{i} is the saturation capacity in $cm^3\ g^{-1}$, and K_{i} is the Langmuir affinity constant expressed in atm^{-1}. The fitting of the isotherm models was achieved by calculating the K_{i} and V_{i} parameters using the solver function in the Microsoft Excel software to minimize the least square difference between experimental and calculated V_{ads}.

For CO adsorption, the two first components in the triple-site Langmuir equation are assigned to high energy and selective adsorption processes due to CO binding to the cobalt atoms, while the third Langmuir component described the physisorption of CO by the porosity of the material itself.

Gas adsorption isotherms of CO, CO_2, N_2, and O_2

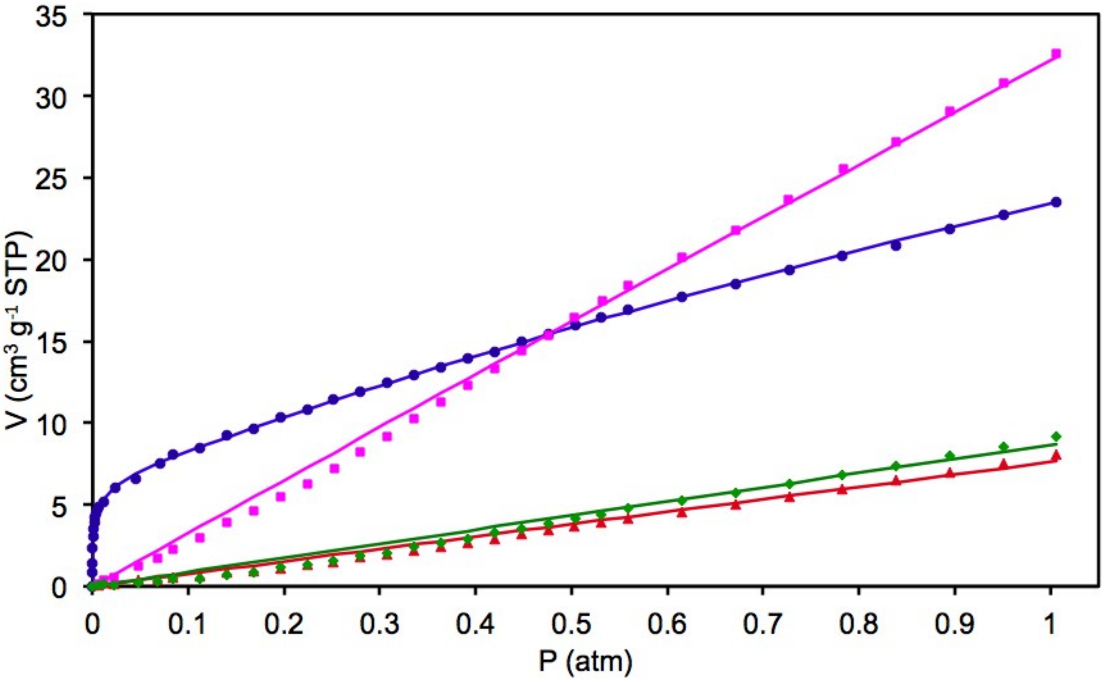

Fig. S18 Adsorption isotherms of CO (blue symbols), CO_2 (pink symbols), N_2 (red symbols) and O_2 (green symbols) recorded at 298 K for **POP-CorCo-1**. Solid lines represent fitting curves using a single-site Langmuir model for N_2, O_2 and CO_2, and a triple-site Langmuir model for CO (see equations (1) and (2) and Tables S3-S5).

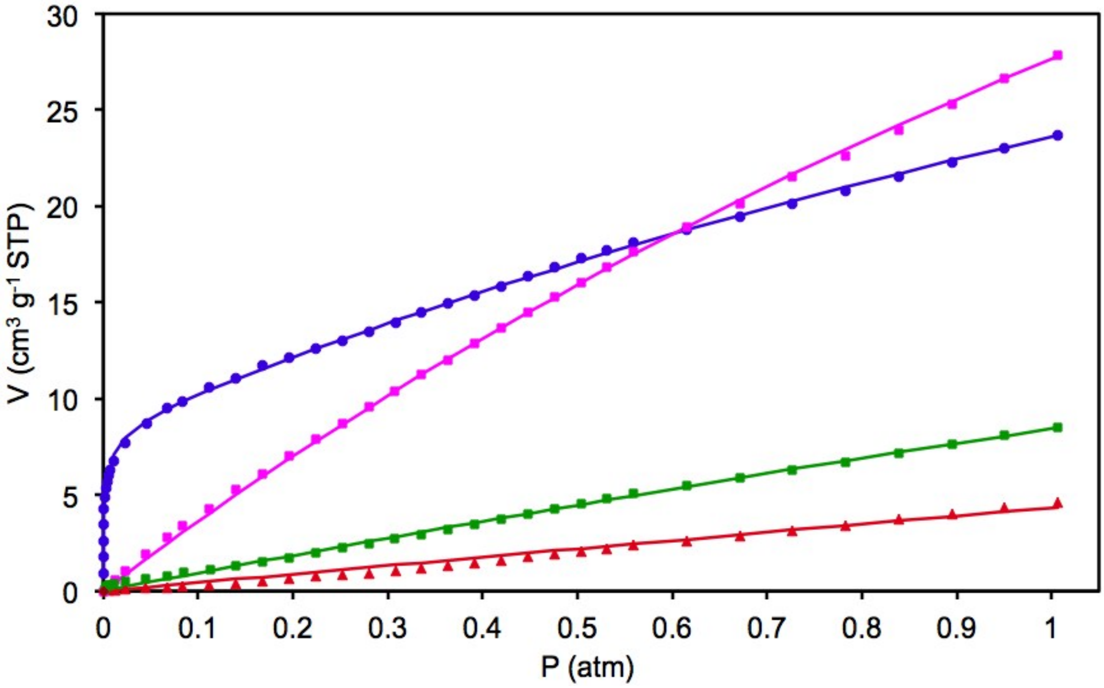

Fig. S19 Adsorption isotherms of CO (blue symbols), CO_2 (pink symbols), N_2 (red symbols) and O_2 (green symbols) recorded at 298 K for **POP-CorCo-2**. Solid lines represent fitting curves using a single-site Langmuir model for N_2, O_2 and CO_2, and a triple-site Langmuir model for CO (see equations (1) and (2) and Tables S3-S5).

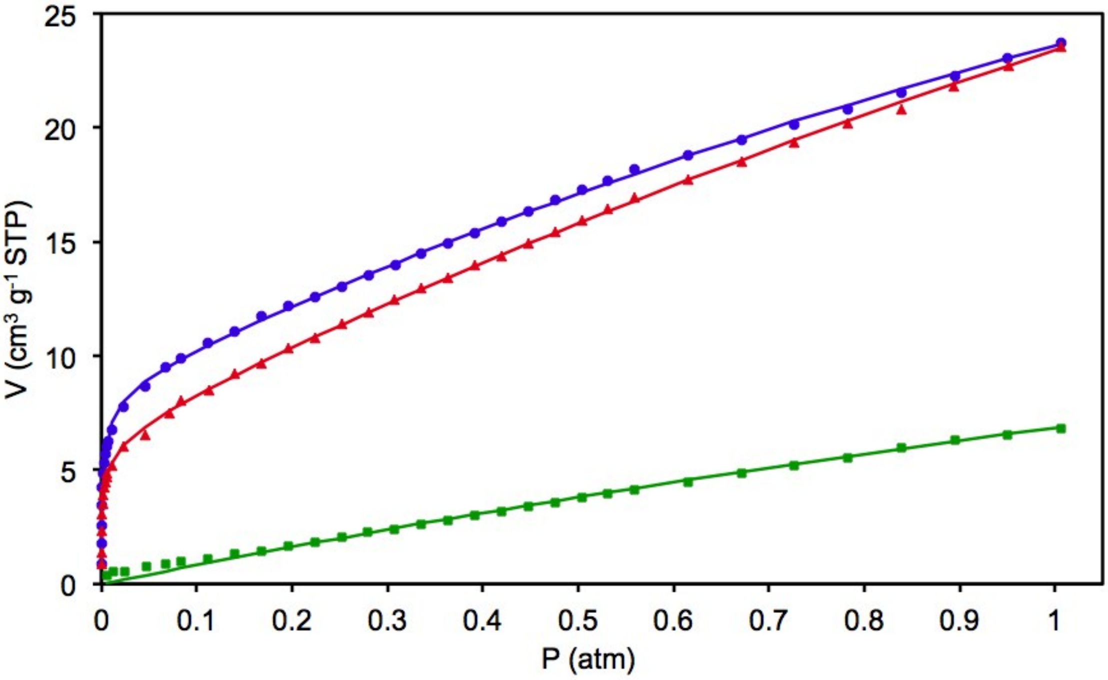

Fig. S20 CO adsorption isotherms for **POP-CorCo-1** (red symbols and curve), **POP-CorCo-2** (blue symbols and curve) and the non-metalated materials **POP-Cor** (green symbols and curve) recorded at 298 K.

Table S3 Summary of gas uptake properties for the two metalated **POP-CorCo-1 and 2**.

Materials	*V_{CO} adsorbed at 1 atm* [a]	*V_{CO} adsorbed at 0.013 atm* [a]	*% active site* [b]
POP-CorCo-1	23.5	5.4	22.7
POP-CorCo-2	23.7	7.2	30.0

[a] Adsorbed volume in cm^3 g^{-1}. [b] Pourcentage of cobalt active sites calculated from the two first components of the Langmuir isotherm model describing the selective CO sorption on cobalt. See Table S4.

Table S4 Fit parameters calculated the CO isotherms recorded at 298 K.

	1st Langmuir component		2nd Langmuir component		3rd Langmuir component		
	V_1 [a]	K_1 [b]	V_2 [a]	K_2 [b]	V_3 [a]	K_3 [b]	$P_{½}^{CO}$ [c]
POP-CorCo-1	3.57	9473	2.89	99.4	87.29	0,241	0.66 10^{-3}
POP-CorCo-2	3.70	18800	4.81	165.6	60.72	0.331	0.92 10^{-3}

[a] Saturation uptakes in cm^3 g^{-1}. [b] Affinity constants in atm^{-1} estimated from triple-site Langmuir model. [c] Half-pressure saturation in atm calculated from the two first Langmuir components describing the selective CO sorption on cobalt.

Table S5 Henry constants[a] calculated from the N_2, O_2 and CO_2 isotherms recorded at 298 K.

	N_2	O_2	CO_2
	V_{N2} [b] x K_{N2} [c]	V_{O2} [b] x K_{O2} [c]	V_{CO2} [b] x K_{CO2} [c]
POP-CorCo-1	7.64	8.69	32.56
POP-CorCo-2	4.49	9.56	37.51

[a] Expressed in $cm^3\ g^{-1}\ atm^{-1}$. [b] Saturation uptakes. [c] Affinity constants estimated from a single-site Langmuir model.

Table S6 Selectivity calculations for CO over N_2, O_2 and CO_2 at 298 K.

	CO / N_2	CO / O_2	CO / CO_2
POP-CorCo-1	4400 [a]	3900 [a]	1050 [a]
	1100 [b]	880 [b]	11 [b]
POP-CorCo-2	15700 [a]	7380 [a]	1880 [a]
	5870 [b]	1670 [b]	35 [b]

[a] Selectivity estimated from the ratio of the Henry constants $H_i = \sum K_i\ V_i$ (= ratio of the initial slopes) at 298 K. [b] Selectivity estimated from the IAST calculations at 298 K and 1 atm assuming mixtures of 0.01% CO in N_2, O_2 or CO_2 (100 ppm CO).

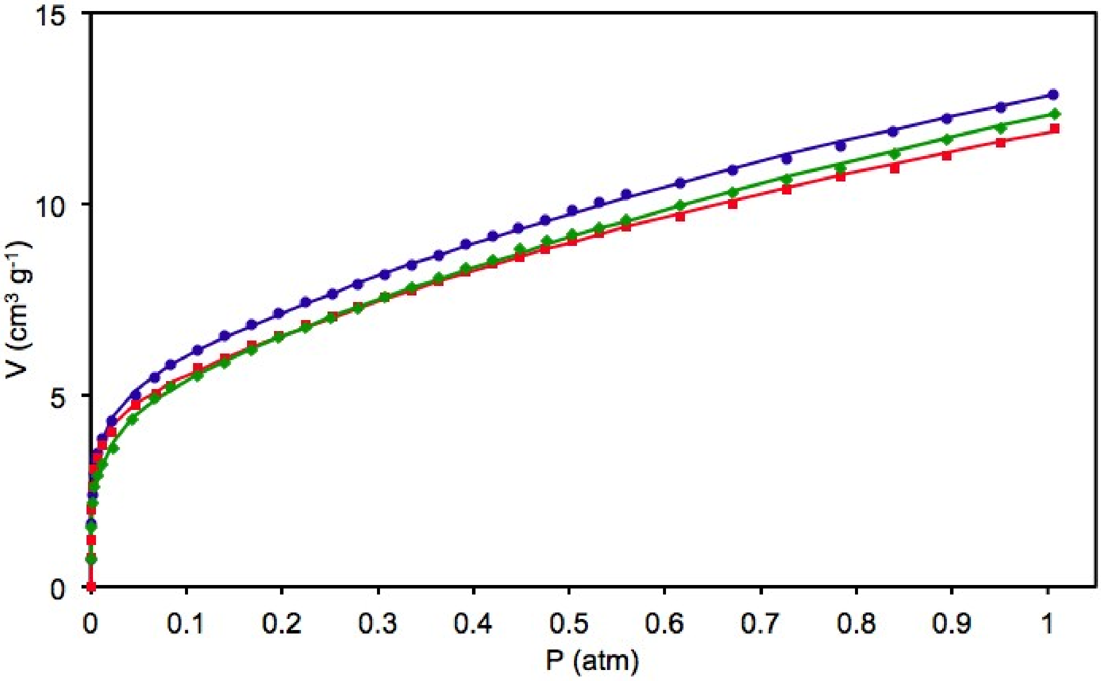

Fig. S21 CO adsorption isotherms for **POP-CorCo-1** recorded at 298 K for three successive cycles (1st cycle: blue symbols; 2nd cycle: red symbols; 3rd cycle: green symbols). The sample was degassed at 80 °C during 3 h between each adsorption measurement.

Calculations of the adsorption selectivities

Selectivities at low coverage were calculated using the constant values resulting from the single- and triple-site Langmuir fits of the experimental isotherms, by determining the Henry constants for each gas (Tables S3 and S5) based on the equation:

$$H_i = \Sigma K_i V_i \qquad (3)$$

The selectivity at zero pressure between gas 1 over 2 is then calculated with the relation:

$$S_{1,2} = \frac{H_1}{H_2} \qquad (4)$$

Reliable information is required to evaluate the efficiency of the materials for gas separation whatever the pressure and the gas mixture. The selectivity for CO over CO_2, N_2 and O_2 in defined binary mixtures were calculated by virtue of the ideal adsorbed solution theory (IAST),[12] that gives a close approximation of a binary gas selective adsorption performance from the experimental single-component isotherms and predicts the gas adsorption selectivity such as CO/CO_2, CO/N_2 and CO/O_2 mixtures in known ratio.[13,14] We have run the calculations assuming CO/gas binary mixture at a molar ratio of 0.01 : 99.99 (100 ppm CO in N_2, O_2 or CO_2) in order to mimic the composition of the polluted gas and this ratio is slightly above the targeted detection level in a sensing device (< 10 ppm).

For IAST calculations (Table S6), the data of the single component isotherms previously obtained from Langmuir fits were used (Tables S4 and S5).

As a thermodynamic criterion to be satisfied to perform the analysis, the spreading pressures of each component are equal to each other ($\pi_i = \pi_j$), π being the spreading pressure calculated by the equation:

$$\frac{a\pi_i}{RT} = \int_0^{p_i^0} \frac{V_i}{p} dp_i \qquad (5)$$

The spreading pressure of component *i* can then be expressed in terms of isotherm parameters using eq (1) and (2). The molar fraction x_i in the adsorbed phase is then determined by the Raoult law:

$$Py_i = P_i^0 x_i \qquad (6)$$

where y_i is the mole fraction in the gas phase and P is the total absolute pressure, P_i^0 corresponds to the partial pressure of the adsorbed phase spreading pressure π_i. The product Py_i corresponds to the partial pressure P_i in the gas phase. π_i is then calculated for each component i and different partial pressure P_i and composition y_i in the gas phase. The adsorption selectivity $S_{1,2}$ for a specific component in a gas mixture is then expressed by:

$$S_{1,2} = \frac{x_1 / y_1}{x_2 / y_2} \qquad (7)$$

In our case, gas compositions have been considered:
CO / Gas (N_2 or O_2 or CO_2): $y_1 = y_{CO} = 10^{-4}$ (100 ppm) and $y_2 = y_{Gas} = 0.9999$.
The calculated selectivities were then plotted as function of the total absolute pressure between 0 and 1 atm as reported in Fig. 5 in the main text.

Adsorption kinetic data

Kinetic of adsorption at low coverage were determined in static conditions at 298 K using the same apparatus used for gas adsorption analyses. The samples were degassed for 2 h before measurements. Starting pressures of 1 or 10 Torr were applied in the manifold before opening the measurement cell. Adsorption kinetic curves are reported in Fig. S24.

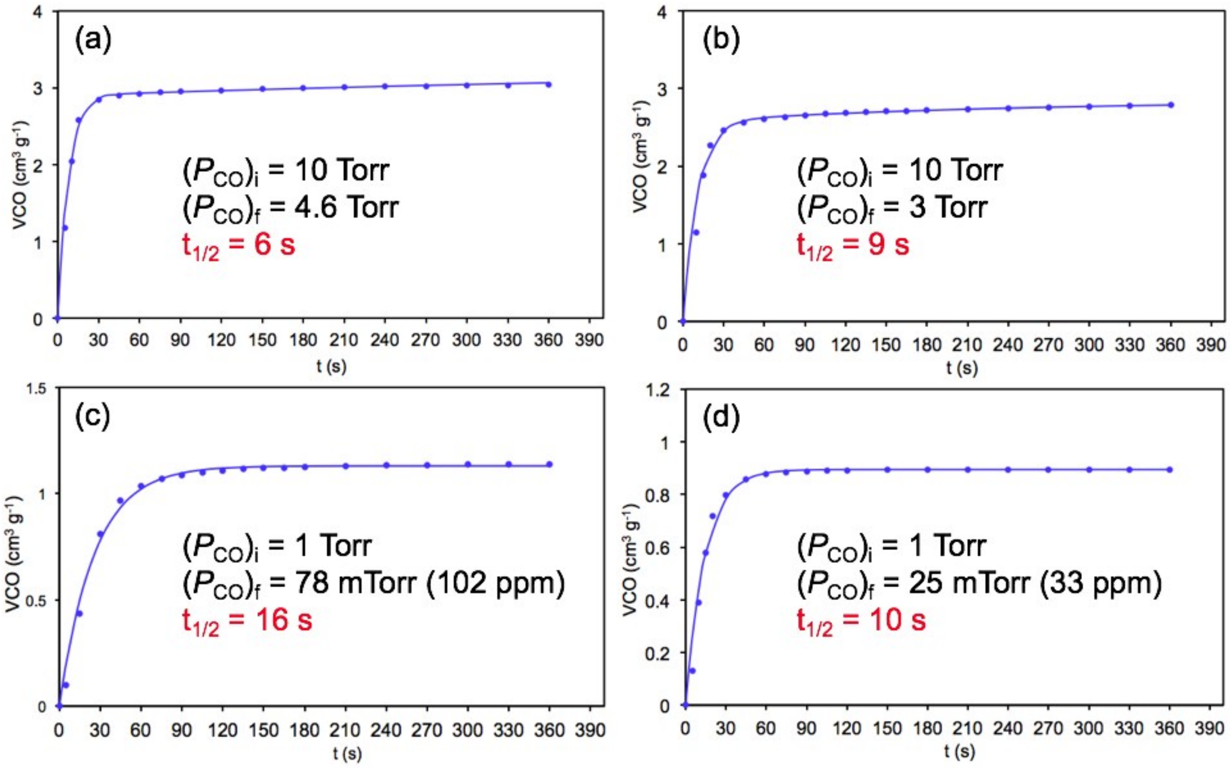

Fig. S22 Kinetic of adsorption recorded in static conditions at 298 K for **POP-CorCo-1** ((a) and (c)) and **POP-CorCo-2** ((b) and (d)) at starting pressures of 1 and 10 Torr.

Adsorption of a gas mixture

Adsorption of a CO/CO_2 gas mixture containing 100 ppm of CO was followed by FTIR spectroscopy for **POP-CorCo-2**. Fig. S23 shows the evolution of the spectra during adsorption and desorption of CO.

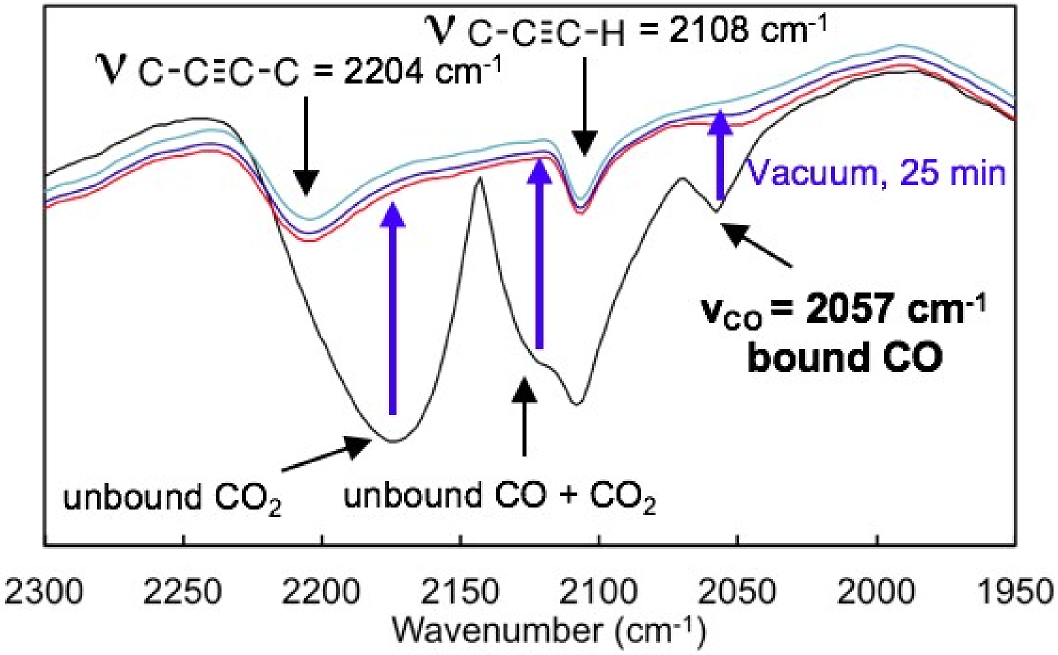

Fig. S23 FTIR monitoring of the adsorption/desorption process recorded for **POP-CorCo-2** after evacuation at 2 mbar followed by exposure for 1 h to a CO/CO_2 gas mixture containing 100 ppm CO. Desorption was recorded under vacuum (30 s → 25 min).

References

1. W. Lu, D. Yuan, D. Zhao, C. I. Schilling, O. Plietzsch, T. Muller, S. Bräse, J. Guenther, J. Blümel, R. Krishna, Z. Li and H.-C. Zhou, *Chem. Mater.*, 2010, **22**, 5964-5972.
2. J. K. Laha, S. Dhanalekshmi, M. Taniguchi, A. Ambroise and J. S. Lindsey, *Org. Process Res. Dev.*, 2003, **7**, 799-812.
3. B. Koszarna and D. T. Gryko, *J. Org. Chem.*, 2006, **71**, 3707-3717.
4. V. Quesneau, W. Shan, N. Desbois, S. Brandès, Y. Rousselin, M. Vanotti, V. Blondeau-Patissier, M. Naitana, P. Fleurat-Lessard, E. Van Caemelbecke, K. M. Kadish and C. P. Gros, *Eur. J. Inorg. Chem.*, 2018, **38**, 4265-4277.
5. K. S. Walton and R. Q. Snurr, *J. Am. Chem. Soc.*, 2007, **129**, 8552-8556.
6. J. Rouquerol, P. Llewellyn and F. Rouquerol, *Stud. Surf. Sci. Catal.*, 2007, **160**, 49-56.

7. B. Wrackmeyer and K. Horchler, *Progress in Nuclear Magnetic Resonance Spectroscopy*, 1990, **22**, 209-253.
8. J. Furrer, S. Guerra and R. Deschenaux, *Magn. Reson. Chem.*, 2011, **49**, 16-22.
9. H. Primasova, P. Bigler and J. Furrer, in *Annual Reports on NMR Spectroscopy*, ed. G. A. Webb, Academic Press, 2017, pp. 1-82.
10. M. Kaupp, O. L. Malkina, V. G. Malkin and P. Pyykkö, *Chem. Eur. J.*, 1998, **4**, 118-126.
11. R. Glaser, N. Chen, H. Wu, N. Knotts and M. Kaupp, *J. Am. Chem. Soc.*, 2004, **126**, 4412-4419.
12. A. L. Myers and J. M. Prausnitz, *AIChE Journal*, 1965, **11**, 121-127.
13. E. D. Bloch, M. R. Hudson, J. A. Mason, S. Chavan, V. Crocellà, J. D. Howe, K. Lee, A. L. Dzubak, W. L. Queen, J. M. Zadrozny, S. J. Geier, L.-C. Lin, L. Gagliardi, B. Smit, J. B. Neaton, S. Bordiga, C. M. Brown and J. R. Long, *J. Am. Chem. Soc.*, 2014, **136**, 10752-10761.
14. D. A. Reed, D. J. Xiao, M. I. Gonzalez, L. E. Darago, Z. R. Herm, F. Grandjean and J. R. Long, *J. Am. Chem. Soc.*, 2016, **138**, 5594-5602.